



Activation of peroxymonosulfate by bicarbonate and acceleration of the reaction by freezing

Yong-Yoon Ahn^a, Jungwon Kim^b, Kitae Kim^{a,c,*}

^a Korea Polar Research Institute (KOPRI), Incheon 21990, Republic of Korea

^b Department of Environmental Sciences and Biotechnology, Hallym University, Chuncheon, Gangwon-do 24252, Republic of Korea

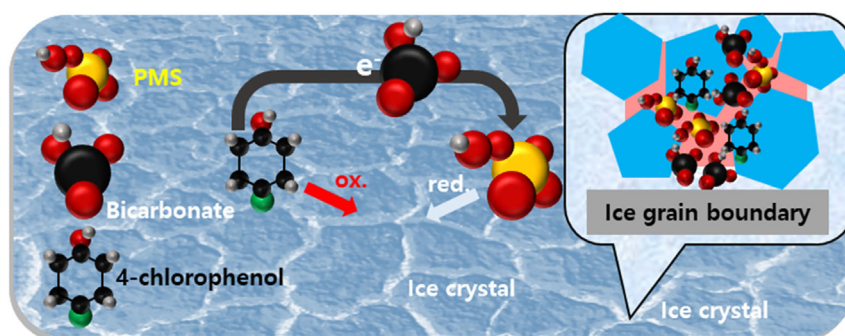
^c Department of Polar Science, University of Science of Technology (UST), Incheon 21990, Republic of Korea



HIGHLIGHTS

- The freezing process was used for enhancing oxidative decomposition of organic pollutant by PMS.
- The positive effects of (bi)carbonate anions on PMS-induced oxidation were studied.
- Remarkable acceleration of the oxidation reaction by freezing was ascribed by freeze-concentration effect.
- The mechanisms of these effects on and acceleration of oxidation were investigated.
- These findings indicate the potential for frozen bicarbonate–PMS water treatment.

GRAPHICAL ABSTRACT



ARTICLE INFO

Article history:

Received 8 March 2021

Received in revised form 20 April 2021

Accepted 22 April 2021

Available online 27 April 2021

Editor: Shuzhen Zhang

Keywords:

Peroxymonosulfate

Bicarbonate

Oxidation

Freeze-concentration effect

Water treatment

Organic pollutant

ABSTRACT

This study demonstrates the positive effects of dissolved bicarbonate and carbonate anions on peroxymonosulfate (PMS) induced oxidation and the remarkable acceleration of the reaction by freezing. More than 90% of the initial 4-chlorophenol (4-CP) decomposed in the frozen case, whereas only less than 20% of the 4-CP was removed in the aqueous case in the same time period. This accelerated reaction is attributed to the freeze-concentration of the dissolved substrates (i.e., PMS, bicarbonate, and pollutants) in the quasi-liquid layer at the ice grain boundaries between ice crystals. The reaction between bicarbonate and PMS was found to be unique because none of the effects were observed in the phosphate and hydroxide cooperated system with freezing, although the base activation of PMS could participate under basic conditions ($\text{pH} > 9$). Based on electron paramagnetic resonance spectroscopy measurements and comparison with the photo-excited Rose Bengal system as a reference system for singlet oxygen ($^1\text{O}_2$) generation, $^1\text{O}_2$ was found to have a minor effect on the oxidation of 4-CP in the frozen bicarbonate–PMS system. While, direct electron transfer from the target organic substrate to the PMS was suggested as a major mechanism of 4-CP oxidation, because the selected target organic substrates were decomposed with different tendencies, and the consumption of PMS was accelerated by the presence of an electron donating compound. The results show the potential applicability of the freezing phenomenon, which occurs naturally in the mid-latitude and polar area, to help a decomposition of water dissolved organic pollutants by the imitation of the natural purification process.

© 2021 Elsevier B.V. All rights reserved.

* Corresponding author at: Korea Polar Research Institute (KOPRI), Incheon 21990, Republic of Korea.
E-mail address: ktkim@kopri.re.kr (K. Kim).

1. Introduction

The significance of temperature in chemical reactions is well known. Specifically, decreasing the temperature decreases the chemical reaction rate. Conversely, the acceleration of certain chemical reactions in the ice phase, which proceed relatively slowly in the aqueous phase, has been identified and studied (O'Concubhair and Sodeau, 2013). These reactions include oxidation of nitrite by dissolved oxygen (Takenaka et al., 1996; Takenaka et al., 1992), redox reactions between chromate and phenolic compounds (Ju et al., 2017), chromate with arsenite (Kim and Choi, 2011), chromate reduction by hydrogen peroxide (Kim et al., 2015), reduction of bromate by humic substances (Min and Choi, 2017), oxidation of inorganic mercury (O'Concubhair et al., 2012), and inorganic peroxide derived oxidation (Choi et al., 2018; Le et al., 2020). Two main circumstances have been postulated to cause acceleration of the reaction in the ice phase; (i) the freeze-concentration effect, and (ii) the freezing-potential effect (O'Concubhair and Sodeau, 2013; Takenaka et al., 1996). The freeze-concentration effect is introduced by the rejection of solutes into the liquid-like region of the ice grain boundary, which is called quasi-liquid layer, from the growing ice crystal. Therefore, the concentrations of solutes in the ice grain boundary are higher than those in the original solution. However, none of the solutes migrate from the ice lattice to the liquid phase with the same degree and tendency; thus, the separation of cations and anions results in electric potential differences, namely, the freezing-potential effect (Workman and Reynolds, 1950). In addition, the catalytic effect of the ice surface and convection during freezing have also been suggested as reasons for acceleration, but the influences of these factors are likely minor relative to those of the two abovementioned features.

Peroxymonosulfate (PMS) is an inorganic oxidant and is widely used in sanitizers, swimming pool cleaners, etchants, and bleaching agents under the commercial name of CAROAT or OXONE. In advanced oxidation processes (AOP), PMS has been used as a precursor of strong oxidizing agents because the homolytic cleavage of the peroxide bond of PMS generates $\text{SO}_4^{\bullet-}$ and $\bullet\text{OH}$ which have redox potentials of 2.4 and 2.7 V_{NHE} respectively (note that the redox potential of PMS is 1.8 V_{NHE}) (Ghanbari and Moradi, 2017; Lee et al., 2020; Wang and Wang, 2018). PMS activation increases the oxidation capability of PMS, and the development of a strategy to activate PMS has become a subject of intensive research for water treatment (Ahn and Yun, 2019). For instance, PMS can be activated by inserting energy in the form of light (Xu et al., 2017), heat (Huang et al., 2017), or ultrasound (Grčić et al., 2012), or via a catalytic reaction using transition metals and noble metals (Ahn et al., 2019), carbon materials (Wang et al., 2017), or a combination of them, such as a photocatalytic reaction (Jo et al., 2018), or electrolysis (Wang et al., 2020). Besides, recent studies showed that the carbonate and bicarbonate can assist metal-catalyzed PMS systems with the degradation of dye compounds (Huang et al., 2016; Dai et al., 2017). Furthermore, Yang et al. reported that bicarbonate ions attack PMS by nucleophilic interaction and increase the Acid Orange 7 decolorization performance (Yang et al., 2010). In the paper, the influence of bicarbonate was identified only in PMS, and no effect of bicarbonate was observed for hydrogen peroxide (H_2O_2) and peroxydisulfate (PDS). The vulnerability of PMS to nucleophilic substances is attributed to the asymmetric chemical structure of PMS.

Bicarbonate is one of the most abundant anion species in natural environments. It has been reported that the bicarbonate concentration of groundwater can vary from 0.7 to 10 mM depending on the regional conditions (Wilkin and DiGiulio, 2010). The concentration of bicarbonate is affected by the pH and the partial pressure of carbon dioxide in the atmosphere. Therefore, it can significantly affect water treatment systems. In general, the role of background species such as bicarbonate in

AOPs has been considered to be retardation because they consume reactive species that are generated by the activation process, and consequently abate the oxidation efficiency (Yang et al., 2017; Mora et al., 2009; Qian et al., 2016; Lee et al., 2018; Ma et al., 2018; Luo et al., 2016; Chen et al., 2018). However, in some cases, the increased removal of organic substances by adding (bi)carbonate to the system has been reported (Nie et al., 2019; Jiang et al., 2017; Sun et al., 2020). The reason for this improvement has been identified as the generation of a selective secondary oxidant, i.e., the weakened secondary oxidant attacks the target organic compound in a more concentrate manner, whereas a strong oxidant (e.g., $\bullet\text{OH}$) can easily be diminished due to its non-selective character. For example, Jiang et al. reported the activation of PDS by bicarbonate in the oxidation of pharmaceuticals, and estimated that the main oxidants are approximately 51.4% singlet oxygen ($^1\text{O}_2$) and 48.6% peroxymonocarbonate (HCO_4^-) (Jiang et al., 2017). Yang et al. reported the positive effect of bicarbonate on the oxidation of organic compounds by PMS, and speculated that HOOCO_2^- species (HCO_4^-) can engage in oxidation (Yang et al., 2018a). Furthermore, carbonate radicals ($\text{CO}_3^{\bullet-}$) can be presumed to be involved in the bicarbonate derived reaction, but there is little information about the involvement of $\text{CO}_3^{\bullet-}$ in the bicarbonate-PMS system (Sun et al., 2020). In fact, we found only limited research on the positive effects of bicarbonate on oxidation, whereas numerous articles have reported negative effects of bicarbonate on AOP systems utilizing PMS (Yang et al., 2017; Mora et al., 2009; Qian et al., 2016; Lee et al., 2018; Ma et al., 2018; Luo et al., 2016; Chen et al., 2018).

In this study, we investigated the reaction of PMS activated by bicarbonate in a frozen solution. We selected 4-chlorophenol (4-CP) as a test organic compound because of its recalcitrant characteristics and toxicity toward aquatic environments (Michałowicz and Duda, 2007). The reaction of PMS and bicarbonate likely caused an oxidative attack on the 4-CP that was accompanied by PMS decomposition, and this reaction was promoted by the freezing process. Because the freezing process obviously enhances the activation of PMS by bicarbonate, we attempted to determine the reason for this enhancement as it is not common knowledge. The oxidation mechanism was investigated by testing plausible scenarios including base activation and the generation of single oxygen molecules and radical species. We also investigated the characteristics of the reaction such as reactivity toward various substrates and the tendency to consume PMS. Although various methods to activate the PMS have been developed, the freezing process does not require an additional input of energy when operated in a cold region.

2. Chemicals and methods

2.1. Chemicals

The chemical reagents used in this study include the following: peroxymonosulfate compound (Sigma-Aldrich, OXONE®), 4-chlorophenol (Sigma-Aldrich), 4-nitrophenol (Sigma-Aldrich), benzoic acid (Sigma-Aldrich), 4-hydroxybenzoic acid (Sigma-Aldrich), phenol (Sigma-Aldrich), hydroquinone (Sigma-Aldrich), furfuryl alcohol (Sigma-Aldrich), Rose Bengal (Sigma-Aldrich), p-benzoquinone (Sigma-Aldrich), sodium bicarbonate (Sigma-Aldrich), sodium carbonate (Sigma-Aldrich), sodium phosphate monobasic monohydrate (Sigma-Aldrich), sodium phosphate dibasic heptahydrate (Sigma-Aldrich), sodium phosphate (Sigma-Aldrich), sodium hydroxide solution (Sigma-Aldrich), perchloric acid (Sigma-Aldrich), hydrogen peroxide solution 30 wt.% (Sigma-Aldrich), methanol (Supelco), acetonitrile (Supelco), formic acid (Sigma-Aldrich), phosphoric acid (Sigma-Aldrich), cresol-red (Sigma-Aldrich), 5-tert-butoxycarbonyl-5-methyl-1-pyrrolidine-N-oxide (BMPO, ENZO Life Science, Inc.), and 2,2,6,6-tetramethylpiperidine (TEMP, Sigma-Aldrich). All chemicals were of reagent grade and were used as received without any further purification. The entire chemical solutions used in this study were prepared with

ultrapure deionized water ($18.2 \text{ M}\Omega \cdot \text{cm}$) which was produced by a Milli-Q Water Purification System (Millipore).

2.2. Experimental procedure

The test solution was prepared in a 100 mL glass beaker. The 100 mM of PMS, NaHCO_3 and Na_2CO_3 stock solutions were added into the beaker to obtain the desired concentration and initial pH value. NaOH and HClO_4 solutions were used if the initial pH was not controlled by the addition of the stock solution. Then, 10 mL of the solution was poured into a 15 mL polypropylene conical tube. Normally, we prepared eight conical tubes, four of which were immersed in an ethanol-circulated cooling bath (operating in -20°C), whereas the remaining four were kept in the atmosphere. The number of conical tubes can be selected according to the time sampling points. These preparation procedures were implemented as fast as possible (approximately 20–30s was required), and we assigned the starting point at this moment (i.e., $t = 0$). After, the conical tube containing the frozen solution was withdrawn from the cooling bath and then put into the 30°C warm water to thaw the ice for conducting chemical analyses. We confirmed that the 4-CP degradation was not derived from the thawing process (Fig. S1). At least two runs of each experiment were performed to confirm the data reproducibility.

2.3. Analytical methods

The concentration of 4-CP was analyzed using a High-Pressure-Liquid-Chromatography (HPLC) (Agilent, 1260 Infinity II). A variable wavelength detector (G7114 1260VWD) was employed and the detection wavelength was set to 230 nm. A Poroshell 120 EC-C18 column ($4.6 \text{ mm} \times 150 \text{ mm}$) was used for separation. The 0.1% (v/v) phosphoric acid and neat acetonitrile were introduced into the pump module (G7111A 1260 Quat Pump VL) to implement isocratic elution (60/40 volume ratio). The oxidation by-products were analyzed using a HPLC (Thermo Fisher Scientific, Vanquish) combined with a quadrupole-orbitrap mass spectrometer (Thermo Fisher Scientific, Q Exactive Focus). The separation was performed on a Hypersil GOLD™ aQ column with a mobile phase composed of 0.1% (v/v) of formic acid (dissolved in LC-MS grade water) and neat acetonitrile (LC-MS grade) at a flow rate of 0.3 mL/min. Mass detection was carried out in a negative electrospray ionization (ESI) mode, and the operating parameters were set as follows: detection range = 50 to 550 m/z with a resolution of 70,000, spray voltage = 2.50 kV, capillary temperature = 320°C , sheath gas flow rate = 40 a.u., auxiliary gas flow rate = 10 a.u., auxiliary gas heater temperature = 300°C , S lens RF level = 50.0, maximum injection time = 200 ms, and an automatic gain control (AGC) target = 1×10^6 . UV-vis spectroscopy (Shimadzu, UV-2600) was used to determine the PMS concentration. The PMS concentration was analyzed using the method proposed by Liang et al., which is based on iodometry (Liang et al., 2008). The on-site detection of concentrated PMS and bicarbonate in frozen solution was conducted using a confocal Raman microscope (Renishaw, InVia Qontor). Liquid sample (25 μL) were dropped onto a silica sample holder ($8 \text{ mm} \times 8 \text{ mm} \times 2 \text{ mm}$) and mounted on a temperature-controlled microscope stage (Linkam Scientific, THMS600). The freezing rate was $-1.5^\circ\text{C}/\text{min}$ and the temperature was maintained at -20°C . The temperature controller was operated using liquid nitrogen and an electrical heating plate. A monochromatic laser ($\lambda = 532 \text{ nm}$ DPSS) was used to introduce Raman-Stokes scattering. The distance from the prism to the 2400 l/mm grating was 8.3 cm. Electron paramagnetic resonance spectroscopy measurements were conducted by using EMXnano (Bruker). The experimental conditions were as follows: Microwave Frequency = 9.64 GHz, Microwave Power = 1 mW, Modulation Frequency = 100 kHz, Modulation Amplitude = 1 G, and Sweep Time = 48 s with continuous-wave-EPR (CW-EPR) mode.

3. Result and discussion

3.1. Degradation of 4-CP in the bicarbonate-PMS system

Fig. 1a shows the degradation of 4-CP by the bicarbonate-PMS system (under aqueous conditions) with the initial PMS dose (black symbols). In the case of a 2 mM PMS dose (at aqueous case), more than half of the initial 4-CP was removed during the 4 h reaction time, where the initial pH was 9. When the PMS dose was decreased to 0.1 mM, the degradation of 4-CP slowed down, i.e., 40%, 20%, and less than 1% of the initial 4-CP decomposed at PMS dose of 1, 0.5, and 0.1 mM, respectively, within 4 h. In addition to the PMS concentration, the 4-CP degradation rate also depends on the concentration of the carbonate species (i.e., the total concentration of HCO_3^- and CO_3^{2-}), as shown in Fig. 1b. It was found that the absence of PMS or bicarbonate caused no degradation of 4-CP, which was followed by a low concentration trend (Fig. S2). Furthermore, reduction of at most 20% of the initial PMS concentration was observed during the reaction in the presence of bicarbonate, whereas no PMS decomposition was detected in the absence of bicarbonate (Fig. S3a). Thus, PMS was activated by bicarbonate, and was responsible for the degradation of 4-CP. This phenomenon agrees well with the recent findings that bicarbonate can be a PMS activator (Nie et al., 2019; Jiang et al., 2017; Sun et al., 2020), although bicarbonate acts as a scavenger of reactive species, therefore, inhibits the oxidation performance in many cases (Yang et al., 2017; Mora et al., 2009; Qian et al., 2016; Lee et al., 2018; Ma et al., 2018; Luo et al., 2016; Chen et al., 2018).

On the other hand, a drastic improvement in 4-CP degradation was found in the ice phase (Fig. 1a; blue symbols). For instance, freezing the solution at -20°C in an ethanol bath resulted in the removal of

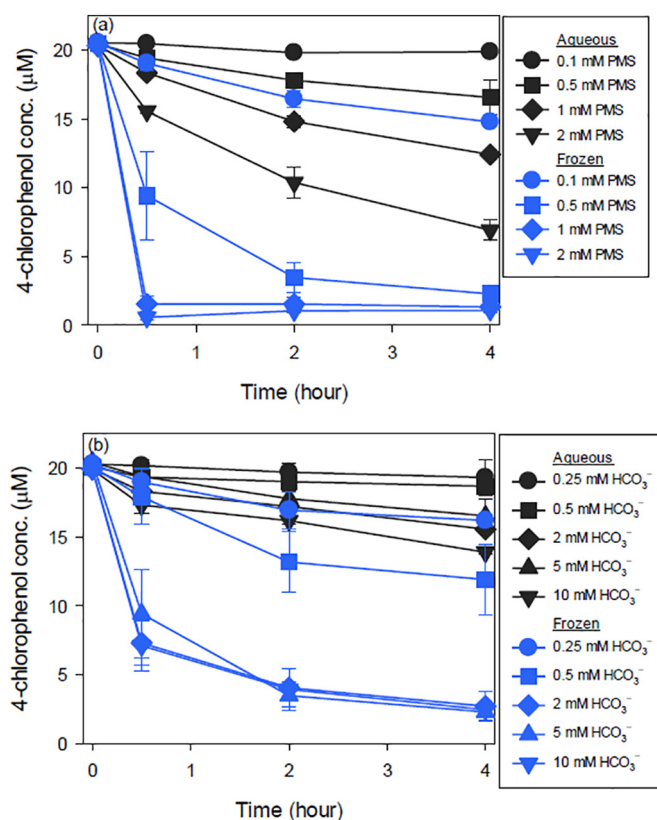


Fig. 1. 4-CP concentration profile versus elapsed time in the bicarbonate-PMS system with (a) various PMS concentrations and (b) various bicarbonate concentrations. $[\text{4-CP}]_0 = 0.02 \text{ mM}$; $[\text{HCO}_3^-]_0 = 5 \text{ mM}$ (at (a)); $[\text{PMS}]_0 = 0.5 \text{ mM}$ (at (b)); $\text{pH}_i = 9$; Temperature = 25°C (aqueous condition) and -20°C (frozen condition).

almost all the 4-CP within 2 h with an initial PMS concentration of 2 mM, while only 50% of the initial 4-CP was decomposed in its aqueous counterpart (Fig. 1a; black symbols). In parallel with this trend, the PMS decomposition rate increased, indicating that 4-CP degradation is highly correlated with PMS consumption (Fig. S3b). According to this, a positive correlation between the initial concentrations of PMS and bicarbonate on 4-CP decomposition rate was also found in the frozen case. From these results, it is clear that the freezing process enhanced 4-CP degradation relative to that under aqueous conditions (Fig. 1).

Because of the arise of freeze-concentration phenomenon during the freezing process, the positive correlation between the PMS (or bicarbonate) concentration and 4-CP removal implies that the freeze-concentration effect is responsible for the acceleration of 4-CP degradation in frozen solution (note that the chemical reaction rate depends on the concentration of the reactants). In this regard, we conducted in-situ measurement of the frozen solution using Raman spectroscopy with a temperature-controllable microscope stage (Linkam, FDSC196). Fig. 2a shows an optical microscope image of the frozen bicarbonate-PMS system focusing on its ice grain boundary, which is an unfrozen region between the ice crystal, along with the Raman spectrum at the marked point. The rainbow scale expression was employed to display the intensity of the Raman scattering light; namely, the red and violet dots represent high and low signals at the position, respectively. Here, the signal at 984 nm was selected for representative intensity of dots. It is obvious that the red and green dots are aligned along the grain boundary,

whereas the bulk of the ice crystal exhibit violet and black dots. In the representative spectrum, the appearance of a specific signal indicates the presence of a particular species, i.e., $\nu = 984 \text{ cm}^{-1}$ likely corresponds to the symmetric S—O stretching vibration and $\nu = 1025 \text{ cm}^{-1}$ probably originated from the C—OH stretching mode of HCO_3^- (Le et al., 2020; Wang et al., 2015; Perkins and Garber, 2003). To confirm these features, we obtained the signals of only PMS or bicarbonate and consequently confirmed that the signals at 883, 984, and 1062 cm^{-1} assigned the PMS whereas that at 1025 cm^{-1} assigned the bicarbonate (Fig. S4 and S5). Evidently, the high intensity of $\nu = 984 \text{ cm}^{-1}$ (i.e., SO_4^{2-}) was concentrated along the ice grain boundary line of the frozen PMS system (Fig. S4). A similar distribution pattern of $\nu = 1020 \text{ cm}^{-1}$ (i.e., HCO_3^-) also manifested when only bicarbonate present (Fig. S5). The absence of PMS and bicarbonate yielded no specific peak even in the center of the grain boundary (Fig. S6). Therefore, we can conclude that the dissolved substrates are accumulate into the ice grain boundary.

We also investigated the influence of the freezing temperature to demonstrate the freeze-concentration effect on the system (Fig. 2b). The point at which freezing began differed along the operated temperature. When the solution was frozen at -10°C , the aqueous phase maintained more than 30 min and the concentration of 4-CP was also retained. This indicates that the oxidation is not initiated before freezing. Similar behavior was observed at -20°C ; at this temperature, approximately 10 min was needed before freezing began. In fact, the

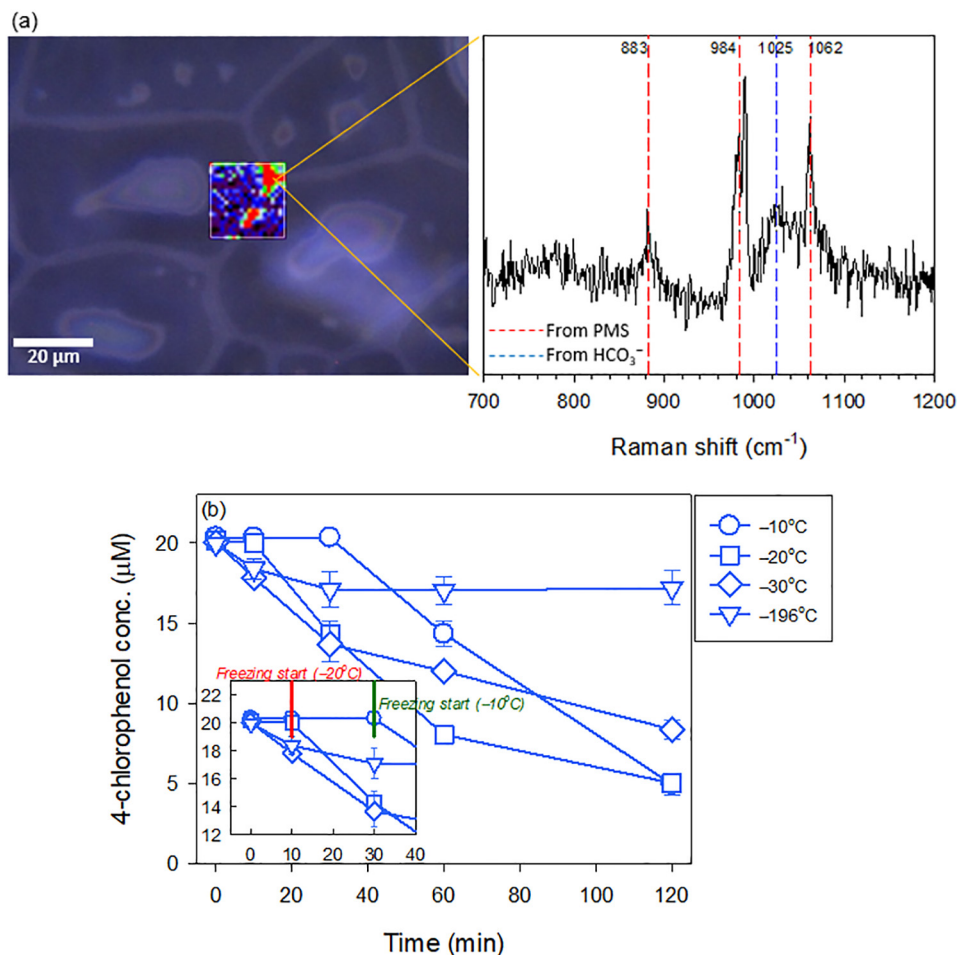


Fig. 2. (a) Microscope image of ice grain boundary and representative Raman spectrum of the frozen bicarbonate-PMS solution. The signal at 984 cm^{-1} was selected to show the map image. Cooling speed = $-2^\circ\text{C}/\text{min}$; terminal temperature = -20°C ; $[\text{PMS}]_0 = 5 \text{ mM}$; $[\text{HCO}_3^-]_0 = 10 \text{ mM}$. (b) 4-CP concentration profile at different freezing temperatures. Temperatures of -10 , -20 , and -30°C were obtained via use of an ethanol bath and that of -196°C was obtained using liquid N_2 . $[\text{4-CP}]_0 = 0.02 \text{ mM}$; $[\text{PMS}]_0 = 0.5 \text{ mM}$; $[\text{HCO}_3^-]_0 = 5 \text{ mM}$; $\text{pH}_i = 9$.

temperature affects both the speed at which freezing occurs and the size of the ice crystals that form (Choi et al., 2018). It is emphasized that when the solution was frozen in liquid nitrogen ($-196\text{ }^\circ\text{C}$), the reaction was evidently retarded owing to the elimination of quasi-liquid layer by amorphously crystallized water at extremely low temperatures. Hence, we can conclude that the freeze-concentration of PMS and bicarbonate occurs in the ice grain boundaries and is responsible for the increased 4-CP oxidation with respect to aqueous case.

3.2. Participation of base-mediated PMS activation in bicarbonate-PMS system

A previous study revealed that PMS spontaneously decomposes in an alkaline environment and that the self-decay is maximized around pH 9.4 (note that the pK_{a2} of PMS is 9.4 and that the peroxide bond of HSO_5^- is readily attacked by nucleophilic SO_3^{2-}) (Yang et al., 2018a). Consequently, the reactions produced SO_4^{2-} and O_2 (i.e., $\text{HSO}_5^- + \text{SO}_3^{2-} \rightarrow \text{HSO}_6^- + \text{SO}_4^{2-}$ and $\text{HSO}_6^- + \text{OH}^- \rightarrow \text{H}_2\text{O} + \text{SO}_4^{2-} + \text{O}_2$) (Ball and Edwards, 1956). In addition, some research has shown that PMS under basic conditions can degrade organic dye compounds and trichlorophenol (Qi et al., 2016; Yang et al., 2018b). Therefore, we examined the influence of base activation as well as the stability of PMS in our system in the aqueous and frozen cases, because our PMS activation system usually conducted at initial pH of 9. Fig. 3 demonstrates the degradation of 4-CP in various pH ranges, which are controlled by three different reagents: carbonate ($\text{HCO}_3^-/\text{CO}_3^{2-}$), phosphate ($\text{H}_2\text{PO}_4^-/\text{HPO}_4^{2-}/\text{PO}_4^{3-}$), and hydroxide (OH^-). Overall, the degradation of 4-CP in all aqueous cases did not exceed 15% of the initial 4-CP concentration at pH 9, and it reached nearly half of that at pH 10 during the 4 h reaction period. Besides, the performance degradation of the NaOH adjusted system was the lowest among the three cases (Fig. 3c). It is noted that PMS decomposition induces a pH shift toward acidic pH values due to H^+ generation (Qi et al., 2016). Apparently, the NaOH adjusted system was sensitively affected by the transformation of PMS (note that the pH was around 7.8 after the reaction when the initial pH was 10; data not shown), while carbonate and phosphate adjusted systems exhibited relatively stable pH variations (with a decrease of 0.5–1 during 4 h of reaction) due to their pH buffering capacities. In addition, there was only a slight loss of PMS in all reagent cases under aqueous conditions on our time scale: the PMS decomposition ratio was not exceeded up of 20% even at an initial pH of 10 (Fig. S7, aqueous cases). Presumably, this PMS decay rate is similar to the previous result if the low ionic strength in our case is considered (Yang et al., 2018a). Accordingly, it is obvious that the base condition affects the PMS system, but this influence is not significant when the pH of the solution is less than 9 under our experimental conditions.

On the other hand, not only the influence of the pH, but also the type of pH adjusting reagent were clearly discriminated in the freezing cases (we need to mention that the initial pH is the value before freezing) (Fig. 3; white symbols). In the carbonate case (frozen, Fig. 3a), 4-CP remains at 65%, 40%, 10%, and <1% of the initial concentration at pH 7, 8, 9, and 10, respectively. It should be emphasized that negligible 4-CP removal appears near a neutral pH when phosphate and NaOH were used for pH adjustment (Fig. 3b, 3c). However, the 4-CP removal reaches 40% when the pH increases to 9 in those two cases. Remarkably, 4-CP is fully eliminated at pH 10 regardless of the reagent type. These results might indicate that the base activation of PMS in the system contributed to the 4-CP removal and improved with freezing. In fact, an acidic solution becomes more acidic during freezing because the local concentration of the acid increases (Heger et al., 2006). Similarly, it is plausible that an accumulation of OH^- occurred during freezing (Takenaka et al., 2006), thereby reinforcing the base activation of PMS and improving the degradation efficiency. To describe this, we employed cresol-red (CR) as pH indicator with which to make in-situ estimation of the pH of the ice. We need to mention that the color of CR was disappeared during freezing when PMS exist in CR solution,

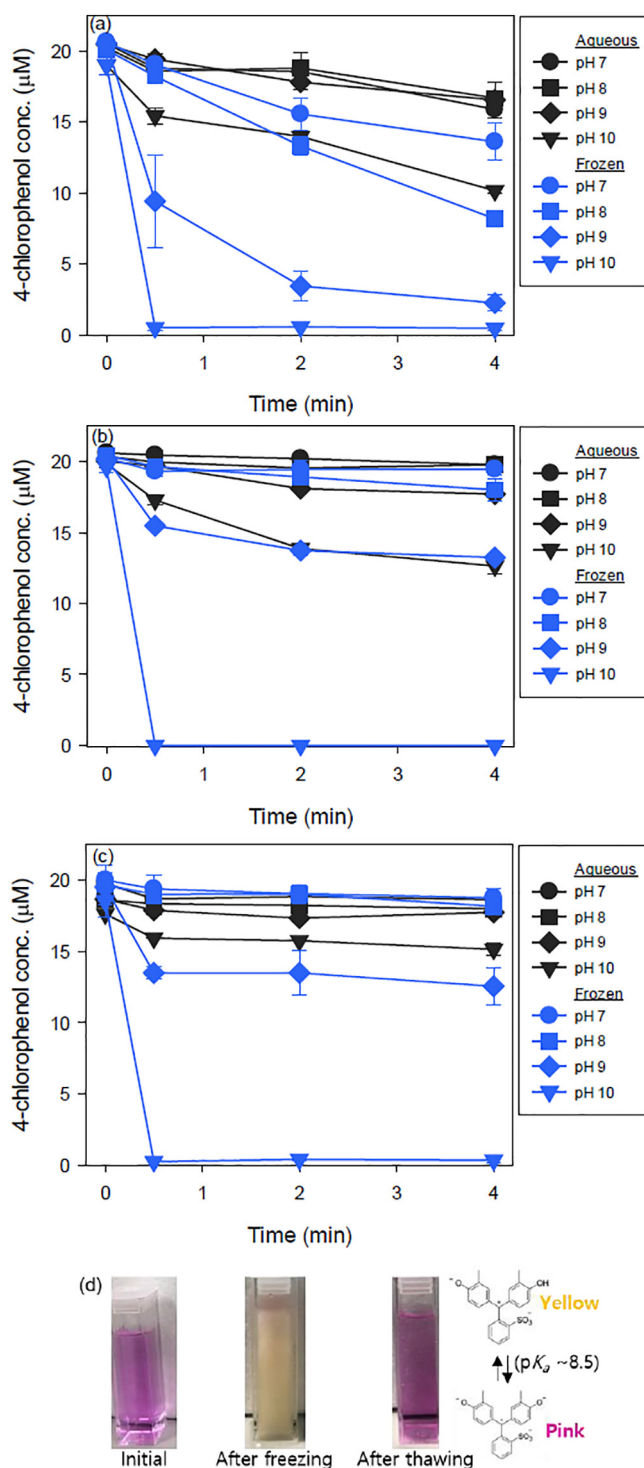


Fig. 3. 4-CP degradation by PMS. The solution pH was adjusted by (a) carbonate, (b) phosphate, and (c) hydroxide anion. $[\text{4-CP}]_0 = 0.02\text{ mM}$; $[\text{PMS}]_0 = 0.5\text{ mM}$; $[\text{anion}]_0 = 5\text{ mM}$; temperature = $25\text{ }^\circ\text{C}$ (aqueous) and $-20\text{ }^\circ\text{C}$ (frozen). (d) The color of cresol-red in the bicarbonate solution. $[\text{HCO}_3^-]_0 = 5\text{ mM}$; $\text{pH}_i = 9$; Freezing temperature = $-20\text{ }^\circ\text{C}$. (For interpretation of the references to color in this figure legend, the reader is referred to the web version of this article.)

due to its oxidation property (data was not shown). For this reason, we prepared bicarbonate solution with an initial pH 9 without PMS. As shown at Fig. 3d, the initial color of CR solution was light pink; however, this changed to light yellow when the solution was completely frozen. The temperature dependence of protonation is not likely significant at this case because the pK_a at 253 K is known to be 8.7 (Heger et al.,

2006); therefore, we believe that the frozen solution has a pH of less than 8.7. Thus, the accumulation of OH^- is not the main reason for the increased PMS activation in the ice. Furthermore, the apparent degradation of 4-CP was also found in the neutral conditions of bicarbonate-PMS system, whereas reactivity in the phosphate and NaOH was marginal (Fig. 3a, 3b, and 3c). Based on the observation, it is likely that some different kinds of chemical reactions occur in the bicarbonate PMS system that do not occur in the phosphate and NaOH systems. In fact, several researchers have reported that the carbonate species in the system can activate PMS to improve the degradation of organic compounds (Yang et al., 2010; Nie et al., 2019; Sun et al., 2020). In this regard, the identification of reactive species is needed to reveal the reaction mechanism.

3.3. Identification of reactive species

As mentioned above, molecular oxygen can be generated during PMS decomposition. In previous research, singlet oxygen ($^1\text{O}_2$) formation via the self-decay of peroxy-acids above their $\text{p}K_a$ value was identified (Evans and Upton, 1985). In addition, according to Zhou et al., the generation of $^1\text{O}_2$ from the reaction of PMS with benzoquinone derived from the intermediate of phenolic compound decomposition was proposed to be the oxidant responsible for organic compound degradation (note that the carbonyl moiety ($\text{C}=\text{O}$) has been found to accelerate $^1\text{O}_2$ production from PMS at basic pH) (Zhou et al., 2017; Zhou et al., 2015). We observed a trend similar to that of Zhou et al., which is the biphasic kinetics of phenol degradation at room temperature (Fig. S10). Therefore, considering the participation of $^1\text{O}_2$ in this stage is quite reasonable. However, electron paramagnetic resonance (EPR) data indicate that the role of $^1\text{O}_2$ in 4-CP degradation is doubtful. As shown in Fig. 4a, we monitored the EPR signal of TEMPO, which was derived from the spin probes TEMP by $^1\text{O}_2$ in our experimental condition, in the bicarbonate-PMS system and base activated (by NaOH) PMS system (Fig. 4a). Apparently, the signal intensity is lower in the bicarbonate-PMS system than in the NaOH-PMS system. Because 4-CP was more efficiently degraded in the bicarbonate-PMS system than in the NaOH-PMS system (Fig. 3), the EPR results indicate that $^1\text{O}_2$ plays a minor role in the 4-CP degradation in the bicarbonate-PMS system. The insignificance of $^1\text{O}_2$ in the 4-CP degradation in our system was also found by comparison with the reference system. Photo-excited Rose Bengal (RB) is a well-known photo-sensitized $^1\text{O}_2$ generation system, so we employed this system to account for the role of $^1\text{O}_2$ (Yun et al., 2018). As shown in Fig. 4b, the degradation of 4-CP was negligible in the photo-excited RB system, while 60% of the 4-CP disappeared in the frozen bicarbonate-PMS system. We confirmed the significant degradation of furfuryl alcohol (FFA), which reacts well with $^1\text{O}_2$ ($k = 1.2 \times 10^8 \text{ M}^{-1}\text{s}^{-1}$ (Scully and Hoigné, 1987)), in the photo-RB system; therefore, $^1\text{O}_2$ likely to arise from photo-excited RB. We need to mention that we adjusted the experimental conditions of the photo-RB system, in which the FFA degradation rate become similar to that in the frozen bicarbonate-PMS case. In parallel with this, the FFA degradation was comparable to (but slightly slower than) the 4-CP degradation in the frozen bicarbonate-PMS system, which means that $^1\text{O}_2$ is not likely a dominant oxidant in the frozen bicarbonate-PMS system.

Peroxymonocarbonate (HCO_4^-) was proposed as another reactive species in the bicarbonate mediated PMS activation. The reactivity of HCO_4^- is weaker (1.8 V_{NHE}) than conventional oxidizing reagents such as $\cdot\text{OH}$ (2.7 V_{NHE}), but numerous papers have suggested that HCO_4^- can oxidize a variety of organic compounds (Xu et al., 2011; Yang et al., 2019; Richardson et al., 2000). Generally, it has been reported that H_2O_2 and HCO_3^- are in chemical equilibrium with HCO_4^- , so we employed the HCO_3^- - H_2O_2 system to estimate the influence of HCO_4^- on the reaction of the bicarbonate-PMS system. However, when we mimicked the experiment of Yang et al. (2019), we observed no disappearance of 4-CP (Fig. 4c), whereas the phenol, which was chosen as target organic pollutant by Yang et al., was decomposed within 120

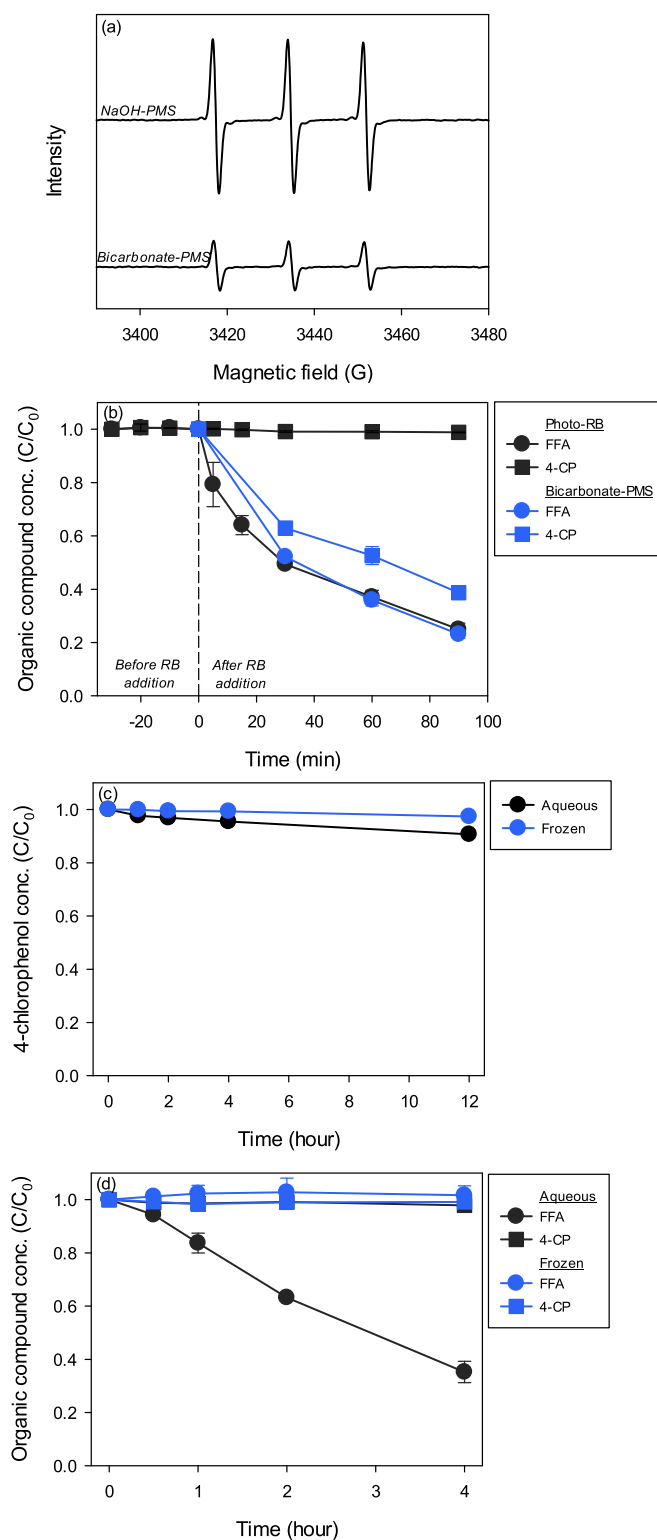


Fig. 4. (a) EPR signal of TEMPO of the frozen PMS solution. NaOH was infused into the PMS solution to make the pH the same as that of the bicarbonate-PMS. $[\text{TEMP}]_0 = 1 \text{ mM}$; $[\text{PMS}]_0 = 0.5 \text{ mM}$; $[\text{HCO}_3^-]_0 = 5 \text{ mM}$ (bicarbonate-PMS); $[\text{NaOH}]_0 = 0.325 \text{ mM}$ (NaOH-PMS); $\text{pH}_i = 9$; Temperature = -20°C . (b) Degradation of organic pollutants in the photo-excited RB and frozen bicarbonate-PMS. In RB systems: $[\text{RB}]_0 = 0.5 \mu\text{M}$; $[\text{HCO}_3^-]_0 = 1 \text{ mM}$. In PMS system: $[\text{PMS}]_0 = 0.5 \text{ mM}$; $[\text{HCO}_3^-]_0 = 5 \text{ mM}$; [organic substrate] $_0 = 0.05 \text{ mM}$; $\text{pH}_i = 9$. (c) Degradation of 4-CP in the bicarbonate activated hydrogen peroxide system. $[\text{H}_2\text{O}_2]_0 = 200 \text{ mM}$; $[\text{HCO}_3^-]_0 = 100 \text{ mM}$; $[\text{4-CP}]_0 = 0.2 \text{ mM}$; $\text{pH}_i = 9$. (d) Degradation of organic pollutants in the bicarbonate-PDS system. $[\text{PDS}]_0 = 5 \text{ mM}$; $[\text{HCO}_3^-]_0 = 5 \text{ mM}$; [organic substrate] $_0 = 0.05 \text{ mM}$; $\text{pH}_i = 9$; temperature = 25°C (aqueous) and -20°C (frozen).

min. In addition, we also found no 4-CP degradation in the bicarbonate-PDS system, which we mimicked the experiment of Jiang et al. (2017), whereas the degradation of FFA was significant in this case (Fig. 4d). Therefore, we speculate that the influence of HCO_3^- on the 4-CP degradation in the frozen bicarbonate-PMS system is negligible.

3.4. Characteristic of the oxidation in the frozen bicarbonate-PMS system

One of the major characteristics of oxidants is their reactivity. Fig. 5 shows the selective oxidation efficacy of the bicarbonate-PMS system. In general, it is known that the split of the peroxide bond in PMS by one-electron transfer results in $\text{SO}_4^{\bullet-}$ generation. The rate constants between $\text{SO}_4^{\bullet-}$ and the test organic compounds at room temperature are reported as follows: 1.2×10^9 (benzoic acid), 2.5×10^9 (4-hydroxybenzoic acid), 8.8×10^9 (phenol), 8.7×10^9 (4-chlorophenol) (Ziajka and Rudzinski, 2007), and 6.83×10^8 (4-nitrophenol) (Rudzinski, 2019). Based on the reaction rate constants, we anticipate that the selected organic compounds can be degraded by $\text{SO}_4^{\bullet-}$ with only slight differences. However, as shown in Fig. 5, the degradation rates of selected organic compounds differ significantly from those in the frozen bicarbonate-PMS system. For instance, benzoic acid was negligibly decomposed, while 4-hydroxybenzoic acid was diminished within 40 min, although the reactivity of the two compounds with $\text{SO}_4^{\bullet-}$ was on the order of $\sim 10^9$. We also confirmed the marginal influence of the addition of an excess of radical quenching agents (Fig. S8). Furthermore, we did not observe a typical signal of spin trapping reagent (5-tert-butoxycarbonyl-5-methyl-1-pyrroline-N-oxide, BMPO) in the EPR spectrum whereas, the benchmark system (i.e., UV/ H_2O_2 as the $\bullet\text{OH}$ system and UV/ $\text{S}_2\text{O}_8^{2-}$ as the $\text{SO}_4^{\bullet-}$ system) showed clear features of radical signals (Fig. S9). Hence, radical species such as $\text{SO}_4^{\bullet-}$ and $\bullet\text{OH}$ were not likely to be reactive species responsible for the oxidation of organic compounds. In addition, we found that 4-hydroxybenzoic acid degraded faster than 4-CP and phenol, which are substituents that have lower electron-withdrawing effects than $-\text{CO}_2\text{H}$ on the aromatic ring. In addition, even though the Hammett constant of 4-nitrophenol (with respect to phenol, $\sigma^+ = 0.79$) is higher than that of 4-chlorophenol ($\sigma^+ = 0.11$) (Lee et al., 2005), it degraded slightly faster than 4-CP in the frozen bicarbonate-PMS system. These findings indicate that the reaction does not rely on the electrophilicity of the aromatic ring. Although we cannot delve into the characteristic of substrate dependence in more detail, it should be emphasized that the oxidation accelerated in the concentrated region in the ice, which requires clarification of the unusual chemical reaction. It is noted that the degradation of selected substrates by bicarbonate-PMS with a reaction time of 1 h was marginal in the aqueous solution, except for that of phenol (Fig. S10).

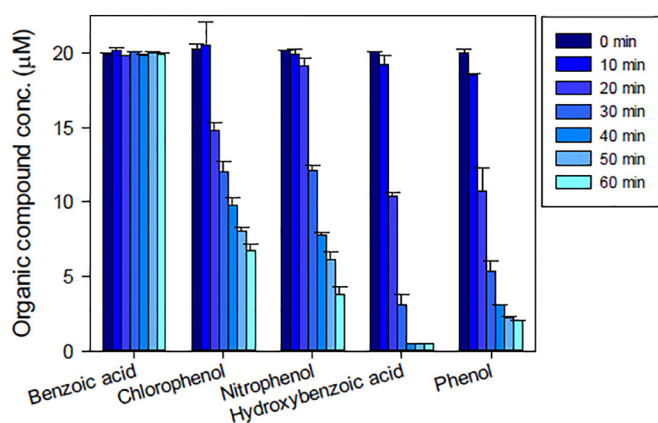


Fig. 5. Degradation of various selected organic compounds in the frozen bicarbonate-PMS system. $[\text{PMS}]_0 = 0.5 \text{ mM}$; $[\text{HCO}_3^-]_0 = 5 \text{ mM}$; $[\text{organic substrate}]_0 = 0.02 \text{ mM}$; $\text{pH} = 9$; temperature = $-20 \text{ }^\circ\text{C}$.

On the other hand, the PMS consumption was strongly related to the degree of organic compound degradation (Fig. 6). The decomposition of PMS in the absence of an organic substrate was comparable to that of benzoic acid, which showed no degradation by the bicarbonate-PMS system. Meanwhile, 4-CP and 4-nitrophenol were moderately degraded PMS, and phenol and 4-hydroxybenzoic acid exhibited fast PMS decomposition. Especially, the addition of hydroquinone resulted in the elimination of PMS within 2 h (Fig. S11). Therefore, we speculated that the electron donating performance of the target organic substrate is closely related to the PMS consumption rate, so direct electron transfer from the electron donor to the acceptor presumably contributed to the reaction. On the other hand, the 40% PMS decomposition in the None case in Fig. 6 was probably caused by the base activation of PMS, which means the generation of $^1\text{O}_2$ from the decomposition of PMS (the presence of $^1\text{O}_2$ was identified from the EPR experiment). Phenol and hydroquinone apparently accelerated the PMS decomposition in aqueous condition (Fig. S12) and were previously reported to be activators to generate $^1\text{O}_2$ from PMS (Zhou et al., 2015). So, this circumstance can concomitantly contribute to the high decomposition of PMS in the phenol and hydroxyquinone cases with respect to the benzoic acid and 4-nitrophenol cases, which are not PMS activator to produce $^1\text{O}_2$.

Parallel to the influence of the target substrate on the PMS decomposition, we found that the increase in bicarbonate dosage also increased the PMS and 4-CP degradation, as shown in Fig. 1b and S3. Also, the absence of bicarbonate showed a very limited 4-CP degradation when the pH was adjusted by phosphate and hydroxide (Fig. 3). All of those reactions became significant in the frozen case rather than the aqueous case (note that freezing induced the freeze-concentration as shown Fig. 2a). In addition, the radical quenching reagent did not inherently degrade 4-CP, and there was no specific EPR signal for $\bullet\text{OH}$, $\text{SO}_4^{\bullet-}$ and $\text{O}_2^{\bullet-}$; therefore, the oxidation mechanism was not likely to have proceeded via a radical species (Fig. S8, S9). With regard to those circumstances, we concluded that electron transfer from the target organic compound to the PMS is likely a primary procedure for oxidation in these cases, as suggested in previous reports (Choi et al., 2018; Le et al., 2020), and bicarbonate ion helps this transfer process. The probability of collision between molecules can be increased during freeze-concentration, promoting electron transfer between reactants. A previous report showed that the coupling reaction between phenolic compounds is more dominant in ice crystals than in aqueous counterparts (Klánová et al., 2003). Similarly, we found that the biphenyl compound, as well as doubly carboxylate compound and sulfonated compound, were more highly evolved in the frozen case, whereas the abundances of some ring-opened compounds were higher in the aqueous case than in the frozen case (Fig. S13). Notably, the generation tendencies of some

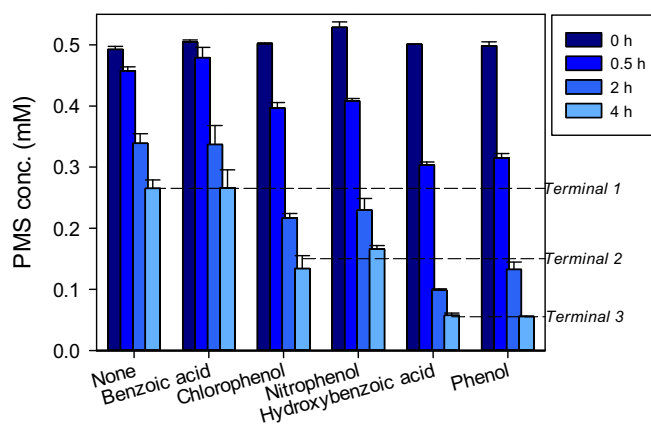


Fig. 6. PMS concentrations obtained using various target organic substrates in the bicarbonate-PMS system with freezing. $[\text{PMS}]_0 = 0.5 \text{ mM}$; $[\text{HCO}_3^-]_0 = 5 \text{ mM}$; $[\text{organic substrate}]_0 = 0.02 \text{ mM}$; $\text{pH} = 9$; temperature = $-20 \text{ }^\circ\text{C}$.

chlorinated intermediates (e.g., chlorocatechol; measured $m/z = 142.98924$) were similar in the aqueous and frozen cases, so they likely share the same degradation pathways in the early stages of the reaction.

4. Conclusion

We investigated the decomposition of 4-CP by a bicarbonate-PMS system and the acceleration of the reaction by freezing. The positive relationship between 4-CP degradation and the concentration of reagents shows that PMS can be activated by bicarbonate. Raman spectroscopy measurements and temperature-dependent experiments suggested that the enhanced 4-CP degradation efficiency in the frozen bicarbonate-PMS system can be ascribed to the freeze-concentration effect. Although the base activation of PMS can affect the degradation of 4-CP, which was induced by a bicarbonate species, the reaction between bicarbonate and PMS was apparent because of the lack of an effect on phosphate and hydroxide system under circumneutral conditions. In addition, observation of the color of CR showed that the pH of ice decreased; therefore, the accumulation of OH^- during the freezing process was not found to be the main reason for the increased PMS activation. The dominant reactive species in the bicarbonate-PMS system was systematically investigated, and a direct electron transfer from organic substances to PMS was proposed to be the main oxidation mechanism. The bicarbonate-PMS reaction was more strongly influenced by the reactant concentrations than the temperature; although the latter is generally an important factor in the reaction. Hence, the bicarbonate-PMS reaction accelerated in the highly concentrated brine in the grain boundary of ice. However, the detailed mechanisms of the reaction of bicarbonate-PMS and that at the concentrated grain boundary are not yet fully understood. Though the mechanism of bicarbonate-PMS has been discussed in some studies, there are still many ambiguities on this issue. The question of how bicarbonate promotes the electron transfer from PMS to the target organic compound remains open and should be studied further. In addition, to reveal the unique properties of chemical reactions during freezing, we will further analyze its characteristics and utility by using various chemical systems.

We also need to mention the environmental implications of the freezing process. Water freezes naturally in cold regions where no external resources are required to make ice. This feature is an advantage of frozen bicarbonate-PMS system, in terms of other processes that induce the PMS activation; heat, ultrasound, and ultra-violet light are energy consuming process that utilize resources to generate the energy required. Furthermore, catalyst-mediated PMS activation processes need post treatment to separate nanomaterials or transition metal ions from the system while the frozen bicarbonate-PMS system does not because all its reagents are natural (e.g., bicarbonate and sulfate). In this regard, our process can be considered as eco-friendly water treatment technology, particularly when it is used in cold areas such as a high latitude region or a mid-latitude in winter. Finally, the frozen bicarbonate-PMS system can degrade various organic pollutants and can thus be expected to function as a potent water treatment system.

CRediT authorship contribution statement

Yong-Yoon Ahn: Conceptualization, Methodology, Writing – original draft. **Jungwon Kim:** Conceptualization, Writing – review & editing. **Kitae Kim:** Conceptualization, Supervision, Validation, Writing – review & editing.

Declaration of competing interest

The authors declare that they have no known competing financial interests or personal relationships that could have appeared to influence the work reported in this paper.

Acknowledgements

This research was supported by the Korea Polar Research Institute (KOPRI) project (PE21120) and was a part of the project titled “Development of potential antibiotic compounds using polar organism resources (15250103, KOPRI Grant PM21030)”, funded by the Ministry of Oceans and Fisheries, Korea.

Appendix A. Supplementary data

Supplementary data to this article can be found online at <https://doi.org/10.1016/j.scitotenv.2021.147369>.

References

- Ahn, Y.-Y., Yun, E., 2019. Heterogeneous metals and metal-free carbon materials for oxidative degradation through persulfate activation: a review of heterogeneous catalytic activation of persulfate related to oxidation mechanism. *Korean J. Chem. Eng.* 36, 1767–1779.
- Ahn, Y.-Y., Bae, H., Kim, H.-I., Kim, S.-H., Kim, J.-H., Lee, S.-G., Lee, J., 2019. Surface-loaded metal nanoparticles for peroxymonosulfate activation: efficiency and mechanism reconnaissance. *Appl. Catal. B Environ.* 241, 561–569.
- Ball, D.L., Edwards, J.O., 1956. The kinetics and mechanism of the decomposition of Caro's acid. *J. Am. Chem. Soc.* 78, 1125–1129.
- Chen, L., Cai, T., Cheng, C., Xiong, Z., Ding, D., 2018. Degradation of acetamiprid in UV/H₂O₂ and UV/persulfate systems: a comparative study. *Chem. Eng. J.* 351, 1137–1146.
- Choi, Y., Yoon, H.-I., Lee, C., Vetráková, L., Heger, D., Kim, K., Kim, J., 2018. Activation of Periodate by freezing for the degradation of aqueous organic pollutants. *Environ. Sci. Technol.* 52, 5378–5385.
- Dai, D., Yang, Z., Yao, Y., Chen, L., Jia, G., Luo, L., 2017. Highly efficient removal of organic contaminants based on peroxymonosulfate activation by iron phthalocyanine: mechanism and the bicarbonate ion enhancement effect. *Catal. Sci. Technol.* 7, 934–942.
- Evans, D.F., Upton, M.W., 1985. Studies on singlet oxygen in aqueous solution. Part 3. The decomposition of peroxy-acids. *J. Chem. Soc. Dalton Trans.* 1151–1153.
- Ghanbari, F., Moradi, M., 2017. Application of peroxymonosulfate and its activation methods for degradation of environmental organic pollutants: review. *Chem. Eng. J.* 310, 41–62.
- Grčić, I., Papić, S., Koprivanac, N., Kovačić, I., 2012. Kinetic modeling and synergy quantification in sono and photooxidative treatment of simulated dyehouse effluent. *Water Res.* 46, 5683–5695.
- Heger, D., Klánová, J., Klán, P., 2006. Enhanced protonation of cresol red in acidic aqueous solutions caused by freezing. *J. Phys. Chem. B* 110, 1277–1287.
- Huang, X., Zhou, X., Zhou, J., Huang, Z., Liu, S., Qian, G., Gao, N., 2017. Bromate inhibition by reduced graphene oxide in thermal/PMS process. *Water Res.* 122, 701–707.
- Huang, Z., Yao, Y., Lu, J., Chen, C., Lu, W., Huang, S., Chen, W., 2016. The consortium of heterogeneous cobalt phthalocyanine catalyst and bicarbonate ion as a novel platform for contaminants elimination based on peroxymonosulfate activation. *J. Hazard. Mater.* 301, 214–221.
- Jiang, M., Lu, J., Ji, Y., Kong, D., 2017. Bicarbonate-activated persulfate oxidation of acetaminophen. *Water Res.* 116, 324–331.
- Jo, Y., Kim, C., Moon, G.-H., Lee, J., An, T., Choi, W., 2018. Activation of peroxymonosulfate on visible light irradiated TiO₂ via a charge transfer complex path. *Chem. Eng. J.* 346, 249–257.
- Ju, J., Kim, J., Vetráková, L., Seo, J., Heger, D., Lee, C., Yoon, H.-I., Kim, K., Kim, J., 2017. Accelerated redox reaction between chromate and phenolic pollutants during freezing. *J. Hazard. Mater.* 329, 330–338.
- Kim, K., Choi, W., 2011. Enhanced redox conversion of chromate and arsenite in ice. *Environ. Sci. Technol.* 45, 2202–2208.
- Kim, K., Kim, J., Bokare, A.D., Choi, W., Yoon, H.-I., Kim, J., 2015. Enhanced removal of hexavalent chromium in the presence of H₂O₂ in frozen aqueous solutions. *Environ. Sci. Technol.* 49, 10937–10944.
- Klánová, J., Klán, P., Nosek, J., Holoubek, I., 2003. Environmental ice photochemistry: Monochlorophenols. *Environ. Sci. Technol.* 37, 1568–1574.
- Le, N.T.H., Ju, J., Kim, B., Kim, M.S., Lee, C., Kim, S., Choi, W., Kim, K., Kim, J., 2020. Freezing-enhanced non-radical oxidation of organic pollutants by peroxymonosulfate. *Chem. Eng. J.* 388, 124226.
- Lee, J., Gunten, U. von, Kim, J.-H., 2020. Persulfate-based advanced oxidation: critical assessment of opportunities and roadblocks. *Environ. Sci. Technol.* 54, 3064–3081.
- Lee, M.-Y., Wang, W.-L., Wu, Q.-Y., Huang, N., Xu, Z.-B., Hu, H.-Y., 2018. Degradation of dodecyl dimethyl benzyl ammonium chloride (DDBAC) as a non-oxidizing biocide in reverse osmosis system using UV/persulfate: kinetics, degradation pathways, and toxicity evaluation. *Chem. Eng. J.* 352, 283–292.
- Lee, Y., Yoon, J., Gunten, U. von, 2005. Kinetics of the oxidation of phenols and phenolic endocrine disruptors during water treatment with ferrate (Fe(VI)). *Environ. Sci. Technol.* 39, 8978–8984.
- Liang, C., Huang, C.-F., Mohanty, N., Kurakalva, R.M., 2008. A rapid spectrophotometric determination of persulfate anion in ISCO. *Chemosphere* 73, 1540–1543.
- Luo, C., Jiang, J., Ma, J., Pang, S., Liu, Y., Song, Y., Guan, C., Li, J., Jin, Y., Wu, D., 2016. Oxidation of the odorless compound 2,4,6-trichloroanisole by UV activated persulfate: kinetics, products, and pathways. *Water Res.* 96, 12–21.

- Ma, J., Yang, Y., Jiang, X., Xie, Z., Li, X., Chen, C., Chen, H., 2018. Impacts of inorganic anions and natural organic matter on thermally activated persulfate oxidation of BTEX in water. *Chemosphere* 190, 296–306.
- Michałowicz, J., Duda, W., 2007. Phenols - sources and toxicity. *Pol. J. Environ. Stud.* 16, 347–362.
- Min, D.W., Choi, W., 2017. Accelerated reduction of bromate in frozen solution. *Environ. Sci. Technol.* 51, 8368–8375.
- Mora, V.C., Rosso, J.A., Roux, G., Carrillo Le, M., Martire, D.O., Gonzalez, M.C., 2009. Thermally activated peroxydisulfate in the presence of additives: a clean method for the degradation of pollutants. *Chemosphere* 75, 1405–1409.
- Nie, M., Zhang, W., Yan, C., Xu, W., Wu, L., Ye, Y., Hu, Y., Dong, W., 2019. Enhanced removal of organic contaminants in water by the combination of peroxymonosulfate and carbonate. *Sci. Total Environ.* 647, 734–743.
- O'Concubhair, R., Sodeau, J.R., 2013. The effect of freezing on reactions with environmental impact. *Acc. Chem. Res.* 46, 2716–2724.
- O'Concubhair, R., O'Sullivan, D., Sodeau, J.R., 2012. Dark oxidation of dissolved gaseous mercury in polar ice mimics. *Environ. Sci. Technol.* 46, 4829–4836.
- Perkins, R.S., Garber, J.D., 2003. Raman spectroscopy of iron in aqueous carbonate solutions. *J. Solut. Chem.* 32, 265–272.
- Qi, C., Liu, X., Ma, J., Lin, C., Li, X., Zhang, H., 2016. Activation of peroxymonosulfate by base: implications for the degradation of organic pollutants. *Chemosphere* 151, 280–288.
- Qian, Y., Guo, X., Zhang, Y., Peng, Y., Sun, P., Huang, C.-H., Niu, J., Zhou, X., Crittenden, J.C., 2016. Perfluorooctanoic acid degradation using UV–Persulfate process: modeling of the degradation and chlorate formation. *Environ. Sci. Technol.* 50, 772–781.
- Richardson, D.E., Yao, H., Frank, K.M., Bennett, D.A., 2000. Equilibria, kinetics, and mechanism in the bicarbonate activation of hydrogen peroxide: oxidation of sulfides by peroxymonocarbonate. *J. Am. Chem. Soc.* 122, 1729–1739.
- Rudziński, K.J., 2019. Aqueous reactions of sulfate radical-anions with Nitrophenols in atmospheric context. *Atmosphere* 10, 795.
- Scully, F.E., Hoigné, J., 1987. Rate constants for reactions of singlet oxygen with phenols and other compounds in water. *Chemosphere* 16, 681–694.
- Sun, Y., Xie, H., Zhou, C., Wu, Y., Pu, M., Niu, J., 2020. The role of carbonate in sulfamethoxazole degradation by peroxymonosulfate without catalyst and the generation of carbonate radical. *J. Hazard. Mater.* 398, 122827.
- Takenaka, N., Ueda, A., Maeda, Y., 1992. Acceleration of the rate of nitrite oxidation by freezing in aqueous solution. *Nature* 358, 736–738.
- Takenaka, N., Ueda, A., Daimon, T., Bandow, H., Dohmaru, T., Maeda, Y., 1996. Acceleration mechanism of chemical reaction by freezing: the reaction of nitrous acid with dissolved oxygen. *J. Phys. Chem.* 100, 13874–13884.
- Takenaka, N., Tanaka, M., Okitsu, K., Bandow, H., 2006. Rise in the pH of an unfrozen solution in ice due to the presence of NaCl and promotion of decomposition of gallic acids owing to a change in the pH. *J. Phys. Chem. A* 110, 10628–10632.
- Wang, G., Chen, S., Quan, X., Yu, H., Zhang, Y., 2017. Enhanced activation of peroxymonosulfate by nitrogen doped porous carbon for effective removal of organic pollutants. *Carbon* 115, 730–739.
- Wang, J., Wang, S., 2018. Activation of persulfate (PS) and peroxymonosulfate (PMS) and application for the degradation of emerging contaminants. *Chem. Eng. J.* 334, 1502–1517.
- Wang, K., Huang, D., Wang, W., Ji, Y., Niu, J., 2020. Enhanced perfluorooctanoic acid degradation by electrochemical activation of peroxymonosulfate in aqueous solution. *Environ. Inter.* 137, 105562.
- Wang, W., Liu, Y., Xue, T., Li, J., Chen, D., Qi, T., 2015. Mechanism and kinetics of titanium hydrolysis in concentrated titanium sulfate solution based on infrared and Raman spectra. *Chem. Eng. Sci.* 134, 196–204.
- Wilkin, R.T., DiGiulio, D.C., 2010. Geochemical impacts to groundwater from geologic carbon sequestration: controls on pH and inorganic carbon concentrations from reaction path and kinetic modeling. *Environ. Sci. Technol.* 44, 4821–4827.
- Workman, E.J., Reynolds, S.E., 1950. Electrical phenomena occurring during the freezing of dilute aqueous solutions and their possible relationship to thunderstorm electricity. *Phys. Rev.* 78, 254–259.
- Xu, A., Li, X., Xiong, H., Yin, G., 2011. Efficient degradation of organic pollutants in aqueous solution with bicarbonate-activated hydrogen peroxide. *Chemosphere* 82, 1190–1195.
- Xu, Y., Lin, Z., Wang, Y., Zhang, H., 2017. The UV/peroxymonosulfate process for the mineralization of artificial sweetener sucralose. *Chem. Eng. J.* 317, 561–569.
- Yang, F., Huang, Y., Fang, C., Xue, Y., Ai, L., Liu, J., Wang, Z., 2018b. Peroxymonosulfate/base process in saline wastewater treatment: the fight between alkalinity and chloride ions. *Chemosphere* 199, 84–88.
- Yang, J.-F., Yang, L.-M., Zhang, S.-B., Ou, L.-H., Liu, C.-B., Zheng, L.-Y., Yang, Y.-F., Ying, G.-G., Luo, S.-L., 2017. Degradation of azole fungicide fluconazole in aqueous solution by thermally activated persulfate. *Chem. Eng. J.* 321, 113–122.
- Yang, S., Wang, P., Yang, X., Shan, L., Zhang, W., Shao, X., Niu, R., 2010. Degradation efficiencies of azo dye acid Orange 7 by the interaction of heat, UV and anions with common oxidants: Persulfate, peroxymonosulfate and hydrogen peroxide. *J. Hazard. Mater.* 179, 552–558.
- Yang, X., Duan, Y., Wang, J., Wang, H., Liu, H., Sedlak, D.L., 2019. Impact of Peroxymonocarbonate on the transformation of organic contaminants during hydrogen peroxide in situ chemical oxidation. *Environ. Sci. Technol. Lett.* 6, 781–786.
- Yang, Y., Banerjee, G., Brudvig, G.W., Kim, J.-H., Pignatello, J.J., 2018a. Oxidation of organic compounds in water by unactivated peroxymonosulfate. *Environ. Sci. Technol.* 52, 5911–5919.
- Yun, E.-T., Lee, J.H., Kim, J., Park, H.-D., Lee, J., 2018. Identifying the nonradical mechanism in the Peroxymonosulfate activation process: singlet oxygenation versus mediated electron transfer. *Environ. Sci. Technol.* 52, 7032–7042.
- Zhou, Y., Jiang, J., Gao, Y., Ma, J., Pang, S.-Y., Li, J., Lu, X.-T., Yuan, L.-P., 2015. Activation of Peroxymonosulfate by benzoquinone: a novel nonradical oxidation process. *Environ. Sci. Technol.* 49, 12941–12950.
- Zhou, Y., Jiang, J., Gao, Y., Pang, S.-Y., Yang, Y., Ma, J., Gu, J., Li, J., Wang, Z., Wang, L.-H., Yuan, L.-P., Yang, Y., 2017. Activation of peroxymonosulfate by phenols: important role of quinone intermediates and involvement of singlet oxygen. *Water Res.* 125, 209–218.
- Ziajka, J., Rudziński, K.J., 2007. Autoxidation of SIV inhibited by chlorophenols reacting with sulfate radicals. *J. Environ. Chem.* 4, 355–363.